NANOSYSTEMS: PHYSICS, CHEMISTRY, MATHEMATICS, 2020, 11 (6), P. 666–671

The novel polyindole based ZnO/MgO nanocomposite adsorbent for the removal of heavy metal ions from industrial effluents

Dedhila Devadathan[1,3], V. Baiju[1,3], J. P. Deepa[2,3], R. Raveendran[1,3]

[1]Nanoscience Research Laboratory, PG & Research Department of Physics, Sree Narayana College, Kollam, India
[2]PG & Research Department of Chemistry, Sree Narayana College, Kollam, India
[3]University of Kerala, India

dedhila@yahoo.com

DOI 10.17586/2220-8054-2020-11-6-666-671

In the present work, ZnO/MgO nanocomposite was synthesized using a co-precipitation method, polyindole and the polyindole based ZnO/MgO nanocomposite were synthesized using chemical oxidation method. The synthesized materials were characterized using XRD and UV/Vis absorbance spectroscopy. The study investigates the applicability of polyindole based ZnO/MgO nanocomposite for the removal of Pb(II) heavy metal ion. Proper tuning can increase the removal efficiency of polyindole based ZnO/MgO nanocomposite and can be made a good candidate for the removal of lead ions.

Keywords: Adsorption, chemical oxidation, co-precipitation, nanocomposite.

Received: 4 August 2020

Revised: 19 October 2020

1. Introduction

Industrialization and urbanization have seriously led to high threat of pollutants like heavy metal ions to public health and environment [1]. So, it was necessary to find a new way to remove heavy metal ions before discharging them into the environment. Due to the economic constraints, development of a cost effective and clean process is essential. The various conventional technologies currently employed in the removal of effluents in industrial water are classical and do not lead to complete removal of pollutants. Therefore, there is a need to develop a novel treatment method that is more effective. Of all the known methods, adsorption has proved to be one of the most effective methods for the removal of heavy metal ions [2]. This method depends on factors such as the surface area, pore size distribution, polarity and functional groups of the adsorbent. Presently, nanotechnology is widely applied for purification and treatment of waste water. The novel properties of nanomaterials such as large surface area, potential for self assembly, high specificity, high reactivity and catalytic potential make them an excellent candidate for this application [3]. A developing trend for the nanomaterials is to synthesize composite structures and devices with materials capable of enhanced properties when compared to counter parts. This can be achieved either by utilizing the size advantage through templating on the nanomaterials and enhancing the properties to drive new synergetic properties of two combined materials [4]. In the present study,a polyindole based ZnO/MgO nanocomposite was prepared, analyzed and used as an adsorbent for the removal of Pb(II) ion. For comparative purposes the counter parts, polyindole and ZnO/MgO were also prepared.

2. Materials and methods

AR grade chemicals obtained from Merck were used for the preparation of ZnO/MgO, polyindole and the polyindole based nanocomposite. ZnO/MgO (ZMF) was prepared by the co-precipitation method in presence of capping agent. Polyindole (PI) and the polyindole based ZnO/MgO nanocomposite (PIZM) were prepared using chemical oxidation method. ZnO/MgO was annealed at 500 °C for three hours; polyindole and polyindole based nanocomposite in the as prepared form were used for analysis. For the preparation of the nanocomposite, ZMF was used. XRD study was carried out using XPERT-PRO model powder diffractometer (PAN analytical, Netherlands) employing Cu-Kα radiation ($\lambda = 1.54060$ Å) operating at 40 kV, 30 mA. The absorbance spectra of these samples were studied using JASCO V 650, UV/Vis spectrophotomer. Adsorption studies in the present work were carried out using GBC-AAS spectrometer having lampcurrent 5 mA and wavelength 270 nm.

3. Result and discussion

3.1. XRD analysis

Figure 1 shows XRD of ZMF. ZMF showed well defined X-ray diffraction peaks which indicated that ZMF had crystalline nature. Again, the broader diffraction peaks indicated the smaller crystallite size. The interplanar spacing (d_{hkl} values), 2θ values and relative intensity values of ZMF corresponding to the observed diffraction peaks were compared with the standard values of ZnO and MgO as reported by JCPDS-International Centre for Diffraction Data. The data obtained for ZnO/MgO matched with JCPDS-ICDD pattern number pattern number #79-0205 of ZnO and #89-7746 of MgO separately. From JCPDS, MgO shows a cubic system with FCC lattice and ZnO shows hexagonal system with a primitive lattice. The presence of peaks of both ZnO and MgO indicates that the prepared sample is not a single phase but a composite. The variation observed in the d values of the crystal planes in case of ZMF when compared to ZnO and MgO from JCPDS, also confirms the formation of composite. The average crystallite size of ZMF calculated from the line broadening of the XRD pattern, using FWHM values of seven major peaks in the XRD spectrum making use of Scherrer formula:

$$D = \frac{k\lambda}{\beta_{hkl} \cos \theta_{hkl}}, \tag{1}$$

where D is the average crystallite size normal to the reflecting planes, k is the shape factor which lies between 0.95 and 1.15 depending on the shape of the grains ($k = 1$ for spherical crystallites), λ is the wavelength of X-ray used and (β_{hkl}) measured is the FWHM of the diffraction line in radians and θ_{hkl} is the Bragg angle corresponding to the diffraction line arising from the planes designated by Miller indices (hkl). The crystallite size for the sample as calculated from Scherrer equation is 22.85 nm. The XRD pattern of PI was found to match well with the XRD patterns in literature [5]. The XRD of polyindole shows the presence of numerous sharp crystalline peaks in the diffraction pattern having 2θ values between 15° and 30°. This can be related to the scattering from bare polymeric chains at the inter-planar spacing. Fig. 2 shows XRD obtained for PI.

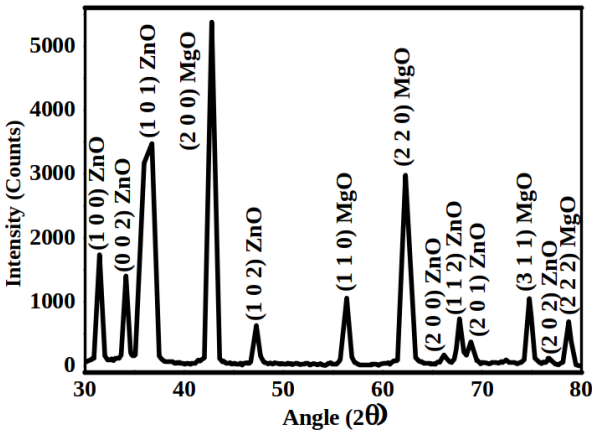

FIG. 1. XRD of ZnO/MgO

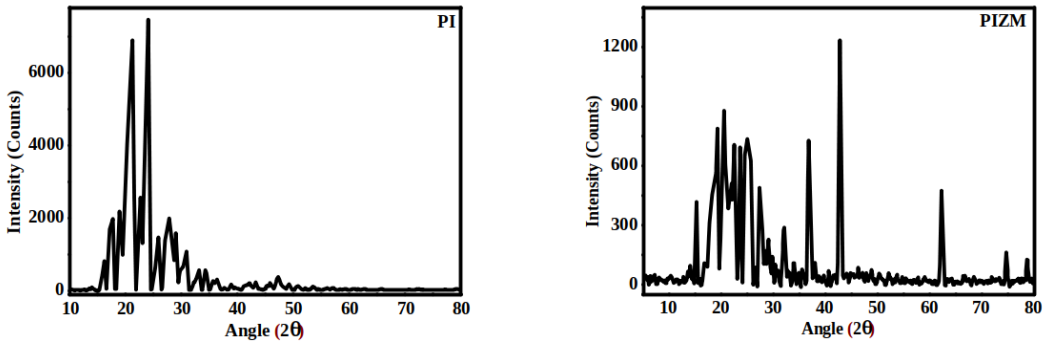

FIG. 2. XRD of polyindole and polyindole based ZnO/MgO nanocomposite

The appearance of peaks in the XRD of the polymer confirms the crystalline nature rather than amorphous nature. The higher the degree of regularity in arrangement or ordering of the polymer chain, the higher is the crystallinity [6]. The presence of sharp crystalline peaks in the XRD graph indicates good electrostatic (dipole–dipole) interactions among the adjoining molecular chains in the PI matrix and also their highly ordered state [7]. The XRD results justify the PI nanostructures as crystalline in nature. Fig. 2 shows XRD obtained for PIZM. XRD of PIZM confirms the formation of nanocomposite. The well defined peaks of planes (1 0 0), (0 0 2) and (1 0 1) of ZnO and (2 0 0), (2 2 0), (3 1 1) and (2 2 2) of MgO were found to be incorporated into the XRD spectrum of polyindole. It is clear from XRD of PIZM that the metal oxide particles are well distributed in the polymer matrix. Here the crystalline peaks between 15° and 30° were also observed. The variation of peaks observed in the XRD of PIZM in the region between 15° and 30° showed variations when compared to the XRD of PI which also supports the formation of nanocomposite.

3.2. UV Analysis

The UV/Vis absorption spectrum of the PI taken in the wavelength range 210 to 800 nm with 1 nm resolution is shown in Fig. 3. PI nanobelts depict a sharp absorption in the range 225 – 325 nm with $\lambda_{\max}$ situated at 292 nm, attributed to the conjugation of the benzenering in the indole unit [8, 9]. The presence of small absorption band is observed in the range 435 – 543 nm with $\lambda_{\max}$ situated at 478 nm due to the $\pi - \pi^*$ transitions of the benzene ring in the PI molecular chains [8]. The results indicate the presence of enhanced conjugated segments and easy flow of charge in PI molecular matrix. This band also relates to the extent of conjugation between adjacent rings in the polymer chain. The optical band gap of the material determined from the absorption spectrum using Tauc's relation was 3.82 eV. Due to large value of the optical band gap, the material is most suited in many applications in modern electronic industries. Fig. 4(a) shows the absorbance spectrum of ZMF. ZMF which displayed sub gaps. The optical band gap of ZMF determined from the absorption spectra using Tauc's relation are 1.75 and 3.3 eV respectively. Fig. 4(c) shows the Tauc plot obtained for ZMF. The UV/Vis absorbance spectrum of PIZM showed multiple absorption peaks in addition to the main peak observed in PI due to $\pi - \pi^*$ transitions in the range 220 – 450 nm with $\lambda_{\max}$ value of 290 nm. The multiple peaks observed in the range 360 to 850 nm could be attributed to the n-π^* and n-π transitions as a result of the interactions between PI chains and ZMF nanoparticles. This causes easy charge transfer from PI to ZMF. The main optical band gap of PIZM determined from the absorption spectra using Tauc's relation was 3.68 eV.

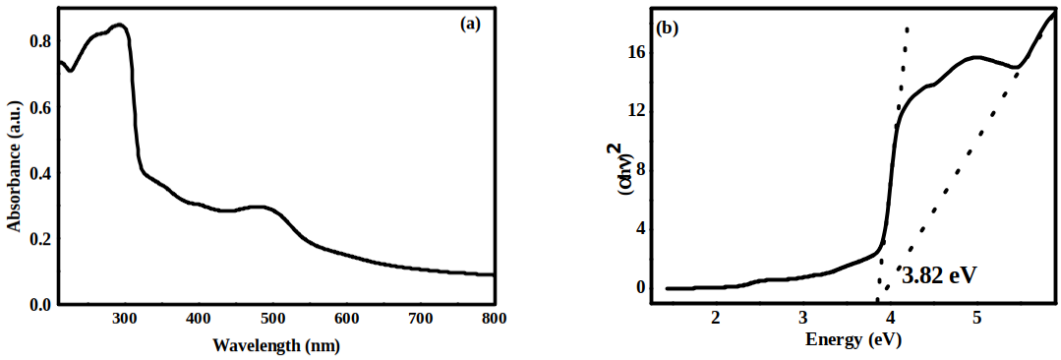

FIG. 3. UV/Vis Absorbance spectrum and (b) Tauc Plot of polyindole

3.3. Adsorption studies

Adsorption studies were performed by batch process by taking 0.1 gm of synthesized ZMF, PI and PIZM in a 100 ml clean and dried stoppered bottle. Known concentration of 50 ml Pb^{2+} solution was added in the same stoppered flask. This flask was placed on a mechanical shaker at 160 rpm and the rate of adsorption of lead on ZMF, PI and PIZM nanocomposite was studied. After desired time intervals (20, 40, 60, 80, 100 min etc.), the solution was filtered using Whatman filter paper no. 41 and reserved for atomic absorption spectroscopy study. The experiments were repeated for different solution pH values. The adsorption capacity (q) and removal percentage are expressed as follows:

$$q = \frac{(C_0 - C_t)\, V}{W}, \tag{2}$$

$$\text{Removal Efficiency } (\%) = \frac{(C_0 - C_e)}{C_0} \times 100, \tag{3}$$

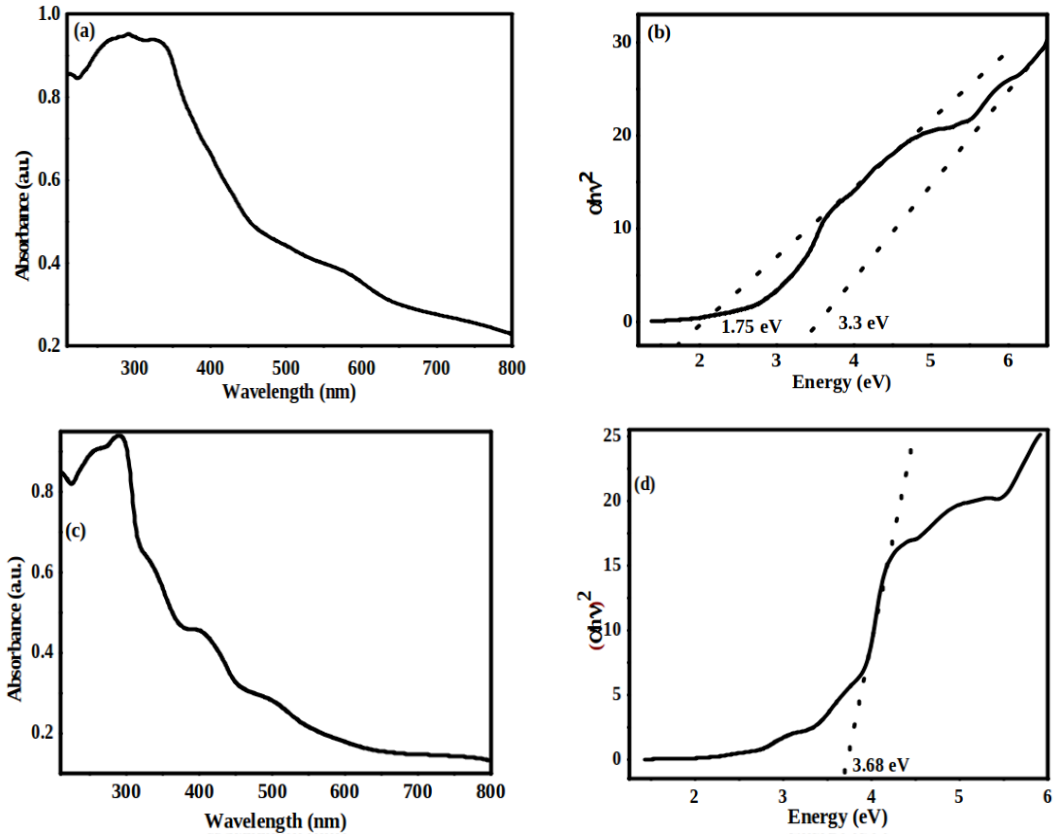

FIG. 4. UV/Vis Absorption spectrum of (a) ZnO/MgO (c) polyindole based ZnO/MgO nanocompositeand Tauc Plot of (b) ZnO/MgO (d) polyindole based ZnO/MgO nanocomposite

where q is the adsorption capacity of the adsorbate (mg·g^{-1}), W is the weight of adsorbent (g), V is the volume of solution (L), and Co (mgL^{-1}) and Ce (mgL^{-1}) are initial and equilibrium concentration of adsorbate in solution.

For the adsorption of Pb^{2+} on the composite PIZM, it was found that the amount of adsorption increased with agitation time and attained equilibrium at 120 minutes i.e., the maximum removal efficiency was attained after 120 minutes (Fig. 5). The removal efficiency of ZMF for Pb^{2+} ions after 120 minutes was found to be 78.56 %. The removal efficiency for polyindole was found to be 62.78 % but, for the nanocomposite, it was 88.98 %.

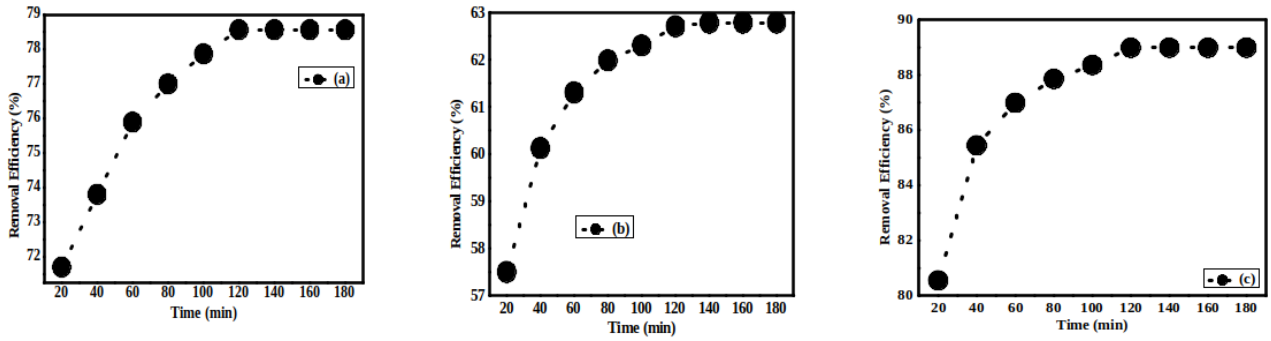

FIG. 5. Removal Efficiency vs Time using ZnO/MgO, polyindole and polyindole based ZnO/MgO nanocomposite for Pb^{2+} adsorption

Polyindole is an organic polymer that holds a large amount of polyfunctional groups (amino and imino groups) that can effectively adsorb heavy metal ions. The development of composite sorbents has opened up new opportunities of their application in deep removal of heavy metals from water. PIZM showed higher adsorption capacity when compared to its counter parts and this can be explained as follows. PIZM has both high specific area due to presence

of metal oxide and functional groups due to the presence of polyindole. In the case of all the three samples, the adsorption was higher in the beginning due to greater number of reaction sites available for Pb^{2+} adsorption.

The pH of the aqueous solution is an important operational parameter in the adsorption process because it affects the solubility of the metal ions, concentration of the counter ions on the functional groups of the adsorbent and the degree of ionization of the adsorbate during reaction [10]. Depending on the pH the active sites on an adsorbent can either be protonated or deprotonated and at the same time the adsorbate speciation in solution also depends the on pH too. Lead for example, exists as Pb^{2+}, $PbOH^{+}$ and $Pb(OH)^{3-}$ depending on the solution's pH.

At lower pH values, low metal ion uptake was observed. The use of a very low pH may result in the competitive adsorption of the H^{+} and Pb^{2+} ions on the PIZM surface. At low pH values, the adsorbent is positively charged due to the presence of H^{+} ions on the surface of adsorbent and hence offers repulsive force to approaching Pb^{2+} ions. However, more Pb^{2+} uptake is observed as the pH increases which are due to the fact that at high pH values, lead still has a net positive charge but exists as $PbOH^{+}$ while most active sites on the adsorbent are deprotonated. This leads to net attractive force that is responsible for high Pb removal from solution in the alkaline pH range.

At elevated pH values; in strong basic solutions, thechances of Pb(II) precipitation increase. It is therefore recommended to operate around the neutral pH to avoid precipitation effect. In the present study, the removal efficiency in the case of all the samples was found to increase with pH and attained maximum at pH 6 and then it was found to decrease (Fig. 6). The nanocomposite, PIZM showed maximum removal efficiency. From the present work it is concluded that proper tuning of PIZM nanocomposite can make it a good adsorbent for the removal of heavy metal ions. Proper tuning can increase the removal efficiency of PIZM and can be made a good candidate for the removal of lead ions.

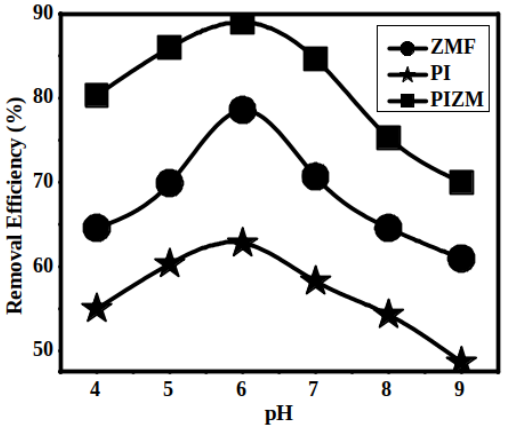

FIG. 6. Removal Efficiency vs pH using ZnO/MgO, polyindole and polyindole based ZnO/MgO nanocompositefor Pb^{2+} adsorption

4. Conclusion

In the present work, ZnO/MgO nanocomposite (ZMF) was synthesized using co-precipitation method; polyindole (PI) and polyindole based ZnO/MgO nanocomposite (PIZM) were synthesized using a chemical oxidation method. The synthesized materials were characterized using XRD and UV/Vis absorbance spectroscopy. The presence of peaks of both ZnO and MgO in ZMF indicates that the prepared sample is not a single phase but a composite.The crystallite size for ZMF, as calculated from Scherrer equation, is 22.85 nm. The appearance of peaks in the XRD of the polymer confirms the crystalline nature rather than amorphous nature of PI. It is clear from XRD of PIZM that the metal oxide particles are well distributed in the polymer matrix. Energy band gaps of all the three samples were calculated from UV/Vis absorbance spectroscopic analysis. The study investigates the applicability of ZMF, PI and PIZM for the removal of Pb(II) heavy metal ion.The removal efficiency of ZMF for Pb^{2+} ions after 120 minutes was found to be 78.56 %. The removal efficiency for polyindole was found to be 62.78 %, but for the nanocomposite, it was 88.98 %, which showed highest removal efficiency. The effect of pH on the removal efficiency of ZMF, PI and PIZM were studied. In the present study, the removal efficiency in the case of all the three samples was found to increase with pH and attained maximum at pH 6 and then it was found to decrease. Proper tuning can increase the removal efficiency of PIZM and can thus be made a good candidate for the removal of lead ions. PIZM was also found to be effective for the removal of Cd^{2+} ions and may possibly be used for the removal of other harmful metal ions, although that remains the scope of a future study.

References

[1] Ngah W.S.W., Hanafiah M.A.K.M. Removal of heavy metal ions from wastewater by chemically modified plant wastes as adsorbents: A review. *Bioresource Technology*, 2008, **99**, P. 3935–3948.

[2] Manohar D.M., Noeline B.F., Anirudhan T.S. Adsorption performance of Al-pillared bentonite clay for the removal of cobalt (II) from aqueous phase. *Applied Clay Science*, 2006, **31**, P. 194–206.

[3] Zhang S., Cheng F., et al. Removal of nickel ions from wastewater by $Mg(OH)_2$/MgO nanostructures embedded in Al_2O_3 membranes. *Journal of Alloys and Compounds*, 2006, **426**, P. 281–285.

[4] Neamtu J., Verga N. Magnetic Nanoparticles for Magneto-Resonance Imaging and Targeted Drug Delivery. *Journal of Nanomaterialsand Biostructures*, 2011, **6**, P. 969–978.

[5] Goel S. Synthesis of polyindole nanoflakes through direct chemical oxidative route. *Advanced Science, Engineering and Medicine*, 2012, **4**, P. 438–441.

[6] Hutten P.F.V., Hadziioannou G. Handbook of Organic Conductive Molecules and Polymers, edited by H.S. Nalwa, John Wiley, New York, 1997, **3**, P. 1–85.

[7] Taylan N.B., Sari B., Unal H.I. Preparation of conducting poly(vinyl chloride)/polyindole composites and freestanding films via chemical polymerization. *Journal of Polymer Science Part B:Polymer Physics*, 2010, **48**, P. 1290–1298.

[8] Eraldemir O., Sari B., Gok A., Unal H.B. Synthesis and characterization of polyindole/poly(vinylacetate) conducting composites. *Journal of Macromolecular Science, Part A: Pure and Applied Chemistry*, 2008, **45**, P. 205–211.

[9] Xu J., Hou J., et al. 1 H NMR spectral studies on the polymerization mechanism of indole and its derivatives. *Spectrochimica Acta Part A*, 2006, **63**, P. 723–728.

[10] Amuda O.S., Ojo O.I., Edewor T.I. Biosorption of Lead from Industrial Waste water using Chrysophyllum albidum seed shell. *Bioremediation Journal*, 2007, **11**, P. 183–194.